Note that Eq. (2) is valid for the following cases:

$$\epsilon_1 \neq \epsilon_2 \quad \epsilon_1 = \epsilon_2 \quad \epsilon_1 \neq \epsilon_2$$
$$H_1 = H_2 \quad H_1 \neq H_2 \quad H_1 \neq H_2$$

That is, the foregoing analysis can be extended to the case of a high (low) local heat transfer coefficient.

Double-Shock Shock Tube for Simulating Blast Loading in Supersonic Flow

Bo Lemcke*
Massachusetts Institute of Technology, Cambridge, Mass.

EXPERIMENTAL simulations of blast loading on moving bodies have been performed mainly in shock tubes until now. Although capable of producing strong shock waves, the shock tube has not been used to establish the interaction between the blast wave and an initial flow on a body. This note will describe a method for obtaining both the initial flow and a blast wave in a shock tube.

It was found by the author[1] that when using a configuration like that shown in Fig. 1, with a large area driver, separated from the shock tube by a diaphragm downstream of the area change, two shock waves appeared at the end of the shock tube. The pressure records obtained were similar to the pressure history indicated on Fig. 2. The explanation for the second shock wave is as follows. When the diaphragm bursts an expansion fan propagates upstream towards the area change. Because of the further supply of driving energy, the rarefaction waves will be reflected as compression waves from the area change, see Fig. 1. The compression waves will converge into a shock wave which will be swept down the expansion tube by the already moving gas. The last compression wave will be generated when the flow in the contraction reaches sonic speed. The further compression behind the second shock wave, indicated in Fig. 2, is due to the arrival of compression waves that have not yet caught up with the shock wave.

To improve the strength and shape of the second shock wave further, it is proposed that another diaphragm be introduced, located at the area change, Fig. 3. This additional diaphragm would make it possible to use different gases and pressures in the two sections of the driver. The configuration utilizing two diaphragms will be called a double-shock shock tube and the different sections the driver, the intermediate driver, and the expansion tube, respectively (see Fig. 3).

The wave pattern in a double-shock shock tube would be slightly different in the early stages from that shown in Fig. 1. It is assumed that the pressure in the driver is of the same order as that in the intermediate driver and that the second diaphragm, located at the area change, cannot withstand a pressure difference that is equal to the pressure in the driver. When the first diaphragm bursts, a rarefaction fan H-T will propagate, as before, up toward the area change. Now, however, it will be reflected from the second diaphragm as a rarefaction wave, thus causing the pressure at the diaphragm to decrease rapidly and eventually forcing it to burst. Thus the second shock wave, S_2, will be formed almost instantaneously at the entrance to the shock tube. If the strength of the second diaphragm is chosen so that the throat becomes sonic immediately, there will be no compression waves following the second shock wave. Thus the introduction of the second diaphragm is expected to make it possible to obtain a well defined second shock wave at a suitable position in the expansion tube. The regulation of the time difference between the two shock waves is affected simply by varying the ratio between the lengths of the intermediate driver and the expansion tube. The flow behind the first shock wave can be used now for establishing steady subsonic or supersonic flow around a body, and the second shock wave can serve as the blast wave for studying the blast loading and the blast wave-bow shock wave interaction.

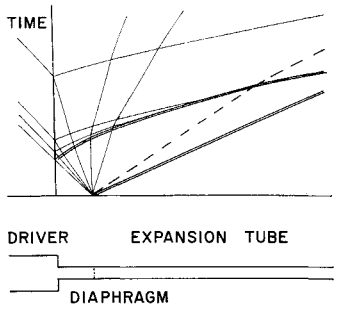

Fig. 1 Configuration used for obtaining two shock waves and the corresponding wave pattern

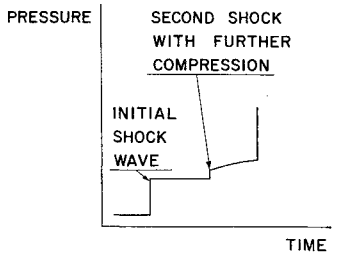

Fig. 2 Obtained pressure record with the configuration indicated in Fig. 1

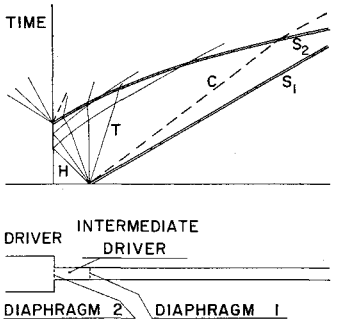

Fig. 3 Wave pattern in double-shock shock tube

To show the capability of the double-shock shock tube one particular case has been worked out by the method of characteristics. The initial conditions were, driver gas: combustion products of 8 He + 3 H_2 + O_2 at 3000 atm;[2] intermediate driver: hydrogen at 2000 atm and 300°K; driver gas: air at 0.2 atm and 300°K. The combustion was assumed to be complete when diaphragm 1 ruptured. Diaphragm 2 was assumed to burst for a pressure difference exactly sufficient to produce a sonic throat at the area change. Real gas effects were taken into account for the shock waves in air. The main results of the calculation were as follows: the stagnation pressure and temperature on a model in the initial flow were 165 atm and 5700°K, respectively; the pressure ratio over the second shock wave after its interaction with the contact surface, C in Fig. 3, was 7.70; the total testing time between the arrival at the end of the shock tube of the first shock wave and the contact surface was about 600 μsec for a 100-ft-long expansion tube.

By changing the gases and pressures in the different sections of the double-shock shock tube a wide range of stagnation conditions on the model as well as blast wave strengths can be simulated. Although the Mach number in the initial flow will be limited to about three, stagnation conditions on the model corresponding to very high velocities at low altitudes can be obtained. Thus the importance of real gas

Received February 25, 1963.

* Senior Research Engineer, Aeroelastic and Structures Research Laboratory.

effects on the transient airloading in the vicinity of the stagnation point of a body already in high-speed flow and then subjected to a blast-type aerodynamic disturbance could be investigated.

References

[1] Lemcke, B., "An investigation of the stagnation conditions in the shock-compression heater of a gun tunnel," Aeronaut. Res. Inst. Sweden Rept. 90 (1962).

[2] Slawsky, Z. J. and Seigel, A. E., "A two-stage driver for shock tubes and shock tunnels (*U*)," U.S. Naval Ordnance Test Station, NAVORD Rept. 5669 (1960).

An Erroneous Concept Concerning Nonlinear Aerodynamic Damping

CHARLES H. MURPHY*
Ballistic Research Laboratories,
Aberdeen Proving Ground, Md.

IN recent years, considerable interest has developed in the aerodynamic damping of symmetric configurations particularly those suitable for re-entry vehicles. Refined rigs have been developed in a number of this country's wind tunnels to measure this quantity for a wide variety of shapes. In most of these experiments, a model is forced to oscillate in a plane about a pivot support in a wind tunnel test section and the energy required to maintain this planar motion is measured and used to obtain values of $C_{M_q} + C_{M_{\dot\alpha}}$. Amplitude dependence can be determined either by forcing oscillations of different amplitudes about zero angle or forcing small-amplitude oscillations about a series of different trim angles.

In the course of this work, it has been noted that, for a large class of shapes at certain Mach numbers, the damping in pitch coefficients changes from destabilizing (positive values) at small amplitude to stabilizing (negative values) at large amplitudes. These data lead to the prediction that a freely oscillating missile should perform a limit oscillation with a fixed maximum amplitude. This is certainly true for a missile constrained to oscillate in a plane; indeed, these oscillations have been observed in tunnel tests. From this, the intuitively "obvious" statement has been made that missiles with this type of planar damping characteristics which are free to perform combined pitching and yawing motion will exhibit a limit cycle motion with a fixed maximum amplitude. It is the purpose of this note to show the fallacy of this assumption by use of a simple counter example.

The aerodynamic moment usually is assumed to be a function of the angles of attack and side slip α, β, the pitching and yawing angular velocities q, r, and the derivatives of these four quantities. For transient oscillations about the flight path, the angular velocities can be eliminated in the moment expansion by the approximations $\dot\alpha = q$, $\dot\beta = -r$. It can be shown that the assumption of rotational symmetry requires that the aerodynamic coefficients are functions of $\delta^2 = \alpha^2 + \beta^2$, $(\delta^2)^{\cdot}$, and $(\dot\alpha)^2 + (\dot\beta)^2$ and that of thesix possible cubic terms in the moment expansion two have a strong effect on the damping of the motion.[1] These two nonlinear terms will be used in our counter-example†; therefore,

$$C_m + iC_n = -i\left\{C_{M_\alpha}\xi + [C_{M_{q_0}} + C_{M_{\dot\alpha_0}} + a\delta^2]\xi' + b(\delta^2)'\xi\right\} \quad (1)$$

where

$$\xi = \beta + i\alpha \qquad \xi' = \dot\xi(l/V) \qquad (\delta^2)' = (\delta^2)^{\cdot}(l/V)$$

In Eq. (1), the first cubic damping moment term induces rotation about an axis normal to the derivative of the complex angle of attack while the second cubic term induces rotation about an axis normal to the complex angle of attack. For planar motion, $\xi = \delta e^{i\theta_0}$ and the complex angle of attack is directed along the same line as its derivative. Therefore,

$$C_m + iC_n = -ie^{i\theta_0}\left\{C_{M_\alpha}\delta + [C_{M_{q_0}} + C_{M_{\dot\alpha_0}} + (a + 2b)\delta^2]\delta'\right\} \quad (2)$$

Note that wind tunnel tests would measure the combination $a + 2b$. For circular motion, however, $\xi = \delta_0 e^{i\theta}$ and the complex angle of attack is normal to its derivative.

$$C_m + iC_n = -i\delta_0 e^{i\theta}\left\{C_{M_\alpha} + i\theta'[C_{M_{q_0}} + C_{M_{\dot\alpha_0}} + a\delta_0^2]\right\} \quad (3)$$

The differential equation for ξ for constant drag, linear normal force, and the moment defined by Eq. (1) is

$$\xi'' + H_0[(1 + A\delta^2)\xi' + (\tfrac{1}{2})B(\delta^2)'\xi] - M\xi = 0 \quad (4)$$

where

$$H_0 = \rho Sl/2m[C_{N_\alpha} - 2C_D - k_t^{-2}(C_{M_{q_0}} + C_{M_{\dot\alpha_0}})]$$
$$A = -(\rho Sl/2m)k_t^{-2}H_0^{-1}a$$
$$B = -2(\rho Sl/2m)k_t^{-2}H_0^{-1}b$$
$$M = (\rho Sl/2m)k_t^{-2}C_{M_\alpha}$$

Under the quasi-linear assumptions,[2] the actual nonlinear angular motion is approximated by a pair of rotating, exponentially damped two-dimensional vectors whose damping exponents are functions of amplitude. Therefore,

$$\xi = K_1 e^{i\phi_1} + K_2 e^{i\phi_2} \quad (5)$$

where

$\phi_j = \phi_{j0} \pm (-M)^{1/2}s$
$K_j' = K_j\lambda_j(K_1^2, K_2^2)$
s = dimensionless arclength ($ds/dt = v/l$)

The general behavior of the motion can be obtained by the study of the $K_1^2 - K_2^2$ plane associated with Eq. (4) (the amplitude plane):

$$\frac{dK_2^2}{dK_1^2} = \frac{K_2^2\lambda_2}{K_1^2\lambda_1} = \frac{K_2^2[1 + BK_1^2 + AK_2^2]}{K_1^2[1 + AK_1^2 + BK_2^2]} \quad (6)$$

The motion described by Eq. (5) is a damped elliptical motion. Points on the coordinate axes of the amplitude plane ($K_1^2 = 0$, or $K_2^2 = 0$) represent circular motion and points on the line $K_1^2 = K_2^2$ correspond to planar motion. When A is negative, circular singularities exist at $(-A^{-1}, 0)$ and $(0, -A^{-1})$; when $A + B$ is negative, a planar singularity exists at $[-(A + B)^{-1}, -(A+B)^{-1}]$. The usual tests for the nature of a singularity[3] show that the planar singularity is a saddle point when

$$-1 < -A/B < 1 \quad (7)$$

and is a node otherwise.

For the lower half of this interval ($-1 < -A/B < 0$), a circular singularity also exists and is a node. This interval on $-A/B$ was used in Ref. 1 in order to illustrate the existence of circular limit motions. If $-A/B$ is in the upper half of this interval, circular and planar singularities cannot exist at the same time. Figure 1 illustrates this possibility for $A + B$ negative.‡

Received February 28, 1963.

* Aeronautical Research Engineer.

† The cubic term $\xi^2\bar\xi'$ of Ref. 1 can be converted to the form of Eq. (1) by the identity $(\delta^2)'\xi = (\xi\bar\xi)'\xi = \xi^2\bar\xi' + \delta^2\xi'$.

‡ In Ref. 4, Eq. (1) is extended to include a cubic static moment ($C_{M_\alpha} = c_1 + c_2\delta^2$).